JOURNAL OF PROPULSION AND POWER
Vol. 20, No. 5, September–October 2004

Heterogeneous Effects in the Propagation and Quenching of Spray Detonations

Tianfeng Lu* and Chung K. Law†
Princeton University, Princeton, New Jersey 08544

The steady propagation of the one-dimensional detonation wave in heptane/air sprays was computationally studied using detailed chemistry, with emphasis on the effects of droplet heating, vaporization, and drag, as well as momentum and heat loss on the detonation velocity and quenching. Results show strong coupling between these processes and the detonation response, leading to a variety of interesting phenomena such as drag-induced concentration of droplets; interference of thermal runaway by cooling due to droplet vaporization; one-stage vs two-stage ignition; chemical heat release controlled by either Arrhenius kinetics or droplet vaporization; internal vs external loss in causing quenching; nonlinear feedback between integrated loss, chemical heat release, and detonation velocity that is responsible for quenching; and the strong influence of the postshock specific heat of the fuel vapor. Consequently, we show that there exist optimum droplet sizes for higher detonation velocities and wider quenching limits and that, depending on the droplet size, higher droplet loading of the spray can also promote detonation propagation and extend its quenching limits.

Introduction

WHILE much has been learned about the initiation and steady propagation of spray detonations,[1–4] corresponding studies on quenching have been relatively few. It is well established that, when there is no loss of energy or momentum, the Chapman–Jouget (CJ) detonation velocity is independent of the detonation structure and is determined by the initial conditions alone.[5] Furthermore, the adiabatic CJ velocity of spray detonation is only slightly lower than that of the corresponding gaseous detonation.[6] However, when loss occurs, the velocity deficit can become substantial and an analysis of the detonation structure is required for the determination of the detonation velocity.[7] In particular, detonation in a gaseous mixture with loss was numerically studied using detailed chemistry[8] and analyzed with a one-step overall reaction.[7–10] Sources of loss include the friction and heat loss, and the curvature effect for a freely expanding wave. Results showed that the reduction in detonation velocity is proportional to the induction length and the extent of the loss during the induction period preceding the state of ignition runaway. Characteristic extinction turning points were obtained,[7] yielding a definitive identification of the state beyond which steady propagation of the detonation is not possible.

The effects of the induction length and loss on detonation in sprays are expected to be more complex due to the additional processes of droplet drag, heating, and vaporization. Sichel and coworkers[11,12] analyzed the one-dimensional structure of two-phase detonations with heterogeneous burning, whereas Ju and Law[10] studied two-phase detonation quenching with substantial particle heating and loss. For spray detonation, the high volatility of the liquid can render strong coupling between vaporization and ignition runaway in that the vaporization process simultaneously lowers the temperature of the induction region and enriches it with fuel vapor.[13,14] The former tends to retard the chemical reaction and increase the induction length whereas the latter facilitates ignition. It is also of interest to distinguish between loss processes that are internal and external to the spray interior. The "loss" from the gas phase due to droplet drag, heating, and vaporization will be returned to it when the droplets are completely vaporized and, as such, can be considered to be internal loss.[15] On the other hand, momentum and heat loss to the environment and incomplete vaporization beyond the sonic state are external and hence permanent. As a result, the effects of droplet drag and vaporization on the detonation velocity and quenching limit can be quite different from those due to the external loss.

Recognizing the importance of droplet vaporization on spray detonation through its coupling with chemistry, in the present work we have computationally solved the structure of the one-dimensional, steady heptane/air spray detonation with simultaneous determination of the detonation velocity and the state of quenching. We are particularly interested in the dependence of these responses on the various spray parameters such as droplet size, loading, number density, drag, and vaporization rate. In our exploration we aimed to be reasonably realistic with respect to the thermochemical aspects of the detonation process. Heptane was chosen as the fuel for demonstration in the present study because of its relatively well-developed gas-phase chemistry and phase-change properties. Furthermore, detailed chemistry was used in the simulation so that the ignition length of the postshock mixture for various postshock temperatures and pressures can be quantitatively predicted with reasonable confidence. On the other hand, we will not include supercritical "gasification" under high initial and, hence, postshock pressures so that the postshock environment is sufficiently subcritical. Furthermore, we shall restrict the initial droplet sizes to sufficiently small values so that we do not need to consider droplet distortion and shattering. Suffice it to note that the initial pressure used in the present simulation, 0.5 atm, is realistic for aeroengine applications and is close to atmospheric pressure, under which most explosions take place. Regarding the initial droplet size, we have restricted it to at most 20 μm, noting the observation of Eidelman and Burcat[16] that shattering occurs for droplet diameters between 50 and 800 μm. Finally, we do not consider the cellular structure of the detonation, recognizing that a simulation of this nature would bring our computational effort to a much higher level of involvement, which would require the concomitant simplification of other aspects of the model such as chemistry. Furthermore, useful information can be gained from a one-dimensional analysis of the present nature, as exemplified by Zeldovich's gas-phase analysis of the quenching of the gaseous detonation,[7] as well as most theoretical studies on detonation.

We also note that, although the problem can be studied in a transient manner, tracking the initiation of a detonation wave through droplet spray or film with vaporization, drag, heat loss, and detailed chemical reaction as was done in Refs. 3 and 4, the present

Received 1 October 2003; revision received 4 April 2004; accepted for publication 19 April 2004.

*Graduate Student, Department of Mechanical and Aerospace Engineering.

†Robert H. Goddard Professor, Department of Mechanical and Aerospace Engineering. Fellow AIAA.

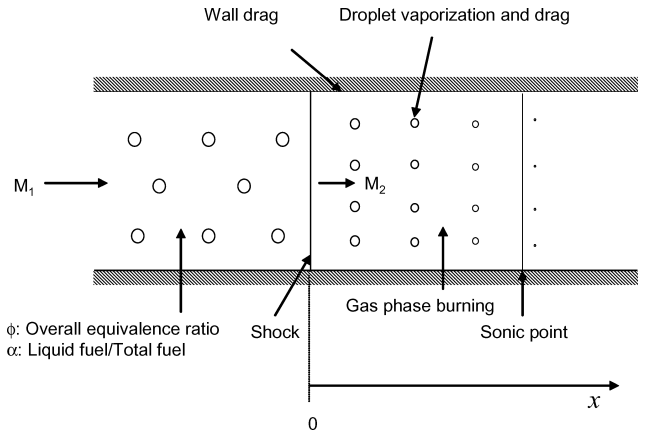

Fig. 1 Schematic of the spray detonation problem analyzed.

steady-state analysis allows a more compact investigation of the influence of the various parameters on the system detonability.

Formulation

The problem being analyzed is schematically shown in Fig. 1. In the one-dimensional detonation stationary frame, a monodisperse spray of initial temperature T_1, pressure p_1, (total) fuel-to-air equivalence ratio ϕ, and droplet radius $r_{d,0}$ passes through an infinitesimally thin shock. The initial droplet number density $n_{d,0}$ can be readily calculated given the preceding parameters. The initial mass fraction of the liquid fuel to the total fuel is designated by the droplet loading parameter α. Upon crossing the shock, the droplets are dragged to slow down from their initial velocity D, which is the detonation velocity, and also start to vaporize. Individual droplet burning is not expected because of the very small droplet sizes of interest,[17] and droplet–droplet or droplet–wall collision and possible coalescence are not considered. Chemical reaction therefore takes place only in the bulk gaseous medium, downstream of the shock, and runs away after an induction period.

The detonation wave loses momentum and energy to the environment. Consequently, in the shock-stationary frame, the wall and droplets drag the flow while heat loss tends to decelerate it. With sufficiently strong loss, chemical runaway cannot accelerate the flow to the sonic state and steady propagation is not possible. Because the analysis is a steady-state one, the solution yields the detonation velocity D when steady propagation is thermochemically possible. The state beyond which such propagation is not possible then yields the state of quenching.

The steady-state governing equations for mass, droplet size, droplet number density, species, momentum, and energy for the planar detonation wave in a single-fuel, monodisperse spray are given by

$$\frac{\mathrm{d}}{\mathrm{d}x}(\rho_g u_g) = \dot{m}_v \tag{1}$$

$$\frac{\mathrm{d}}{\mathrm{d}x}\left(\rho_d n_d \frac{4}{3}\pi r_d^3 u_d\right) = -\dot{m}_v \tag{2}$$

$$\frac{\mathrm{d}}{\mathrm{d}x}(n_d u_d) = 0 \tag{3}$$

$$\frac{\mathrm{d}}{\mathrm{d}x}(\rho_g u_g Y_{g,k}) = \omega_k W_k + \dot{m}_v Y_{d,k} \qquad k = 1, \ldots, K \tag{4}$$

$$\frac{\mathrm{d}}{\mathrm{d}x}\left(p + \rho_g u_g^2\right) = f_d + f_w + \dot{m}_v u_d \tag{5}$$

$$\frac{\mathrm{d}}{\mathrm{d}x}\left(\rho_d n_d \frac{4}{3}\pi r_d^3 u_d^2\right) = -f_d - \dot{m}_v u_d \tag{6}$$

$$\frac{\mathrm{d}}{\mathrm{d}x}\left[\rho_g u_g\left(h_g + \frac{u_g^2}{2}\right)\right] = f_w D - q_w + f_d u_d - q_d + \dot{m}_v\left(h_{g,f} + \frac{u_d^2}{2}\right) \tag{7}$$

$$\frac{\mathrm{d}}{\mathrm{d}x}\left[\rho_d n_d\left(\frac{4}{3}\pi r_d^3\right)u_d\left(h_d + \frac{u_d^2}{2}\right)\right] = q_d - f_d u_d - \dot{m}_v\left(h_{g,f} + \frac{u_d^2}{2}\right) \tag{8}$$

where $h_{g,f} = h_{g,f}(T_d)$ and T_d is the droplet temperature, which is assumed to be uniform. Furthermore, ρ is the density; u is the velocity relative to the shock; n_d is the droplet number density; r_d is the droplet radius; $\dot{m}_v$ is the volumetric mass vaporization rate of the droplets; Y is the mass fraction; ω is the molar reaction rate; W is the molecular weight; f_d is the droplet drag; f_w is the external drag force; D is the detonation velocity; q_w is the external heat loss; q_d is the heat flux for droplet heating; h is the enthalpy; and the subscripts g, d, K, k, and f denote properties of the gas phase, properties of the droplet, the total number of species, the kth species, and the fuel, respectively.

The preceding equations are to be solved subject to the following auxiliary relations:

$$h_g = \sum_{k=1}^{K} h_{g,k} Y_{g,k} \tag{9}$$

$$h_{g,k} = (h_{g,k})_0 + \int_{T_0}^{T} c_{pg,k}\,\mathrm{d}T_g \tag{10}$$

$$p = \rho_g R_g T_g \tag{11}$$

$$f_d = n_d C_{D,d}\left(4\pi r_d^2\right)\rho_g |u_d - u_g|(u_d - u_g)/2 \tag{12}$$

$$C_{D,d} = 22 Re_d^{-1}\left(1 + 0.276 Re_d^{\frac{1}{2}} Pr^{\frac{1}{3}}\right) \tag{13}$$

$$f_w = \frac{C_{D,W}}{l^*}\rho_g |D - u_g|(D - u_g)/2 \tag{14}$$

$$q_w = \frac{C_{H,W}}{l^*}\rho_g |D - u_g| c_{p,g}(T_g - T_w) \tag{15}$$

where c_p is the specific heat; R_g is the universal gas constant; $C_{D,d}$ is the drag coefficient[13]; Pr is the Prandtl number; l^* is the characteristic length; $C_{D,W}$ and $C_{H,W}$ are the momentum and heat loss coefficients, respectively; and Re is the Reynolds number.

In specifying the droplet vaporization process, we note that, because of the high temperature and pressure of the postshock state, droplet heating is expected to be important. Furthermore, the high postshock pressure and the low droplet temperature immediately downstream of the shock imply the potential of fuel vapor condensation onto the droplet. As such, the droplet vaporization, condensation, and heating processes need to be described reasonably realistically[17] instead of following the simple d^2-law with a constant gasification coefficient. Consequently, droplet heating and vaporization are described by the following relations:

$$\dot{m}_v = n_d(4\pi r_d)\frac{\lambda_g}{(Le)c_{p,g}}\ell_n(1 + B_Y)\left(1 + 0.276 Re_d^{\frac{1}{2}} Pr^{\frac{1}{3}}\right) \tag{16}$$

$$q_d = n_d(4\pi r_d)\frac{\lambda_g}{c_{p,g}}\ell_n(1 + B_H)\left(1 + 0.276 Re_d^{\frac{1}{2}} Pr^{\frac{1}{3}}\right)L \tag{17}$$

$$Le = \frac{\lambda_g}{\rho_g c_{p,g} D_g}, \qquad B_Y = \frac{Y_{f,s} - Y_f}{1 - Y_{f,s}}, \qquad B_H = \frac{c_{p,g}(T_g - T_d)}{L} \tag{18}$$

$$Y_{f,s} = Y_{f,s}(p, T_d) \tag{19}$$

where the subscript s denotes the droplet surface, L denotes the latent heat of vaporization, and D_g denotes the mass diffusivity of the gas. It is seen that the droplet vaporization rate is controlled by

the vapor pressure gradient and heat flux at the droplet surface. In the droplet heating stage, B_Y is smaller than B_H, and the heat flux q_d is used for both vaporization and droplet heating. Toward the end of the droplet heating period, B_Y approaches B_H and q_d is almost totally used for vaporization. Equation (19) relates the surface vapor pressure with the droplet temperature, and in the present study is given by the Antoine equation[18]:

$$\log_{10}(p_{f,s}) = A - B/(T_d + C) \tag{20}$$

where $p_{f,s}$ is the fuel vapor pressure at the droplet surface, and A, B, and C are empirically determined constants. Finally, the fuel mass fraction $Y_{f,s}$ and $p_{f,s}$ are related through

$$Y_{f,s} = \frac{X_{f,s}W_f}{X_{f,s}W_f + (1 - X_{f,s})\bar{W}_{g,\bar{f}}}, \qquad X_{f,s} = \frac{p_{f,s}}{p} \tag{21}$$

where $\bar{W}_{g,\bar{f}}$ is the mean molecular weight of the gaseous mixture without the fuel.

We note in passing that an alternate model for droplet heating was presented in Ref. 19, which requires further modeling of the Nusselt number for the determination of the droplet heating flux. Furthermore, although the accuracy for the vaporization rate for small droplets could be improved by accounting for nonequilibrium effects,[20,21] the equilibrium model in Eqs. (16–21) is considered sufficient for the present study considering the uncertainty in other aspects of the problem such as chemistry, drag, and droplet dispersion.

From the governing equations of motion, evolution of the flow variables is given by

$$\frac{\mathrm{d}u_g}{\mathrm{d}x} = \frac{(\gamma - 1)M^2 S}{(M^2 - 1)\rho_g u_g^2} \tag{22}$$

$$\begin{aligned} S = {} & f_w\left(\frac{\gamma}{\gamma - 1}u_g - D\right) + q_w + f_d\left(\frac{\gamma}{\gamma - 1}u_g - u_d\right) + q_d \\ & + \sum_{k=1}^{K}\left[\left(h_{g,k} - c_{p,g}T_g\frac{\overline{W_g}}{W_k}\right)\omega_k W_k\right] \\ & + \dot{m}_v\left\{\frac{\gamma}{\gamma - 1}u_g(u_d - u_g) - c_{p,g}T_g\frac{\overline{W_g}}{W_f} - \frac{\left(u_d^2 - u_g^2\right)}{2}\right. \\ & \left. + [h_{g,f}(T_g) - h_{g,f}(T_d)]\right\} \end{aligned} \tag{23}$$

$$\begin{aligned} \frac{\mathrm{d}T_g}{\mathrm{d}x} = {} & -\frac{u_g}{c_{p,g}}\frac{\mathrm{d}u_g}{\mathrm{d}x} + \frac{1}{\rho_g u_g^2}\left\{f_w D + f_d u_d\right. \\ & - \sum_{k=1}^{K} h_{g,k}\omega_k W_k - q_w - q_d \\ & \left. + \dot{m}_v\left[\frac{u_d^2 - u_g^2}{2} - h_{g,f}(T_g) + h_{g,f}(T_d)\right]\right\} \end{aligned} \tag{24}$$

$$\frac{\mathrm{d}\rho_g}{\mathrm{d}x} = -\frac{\rho_g}{u_g}\frac{\mathrm{d}u_g}{\mathrm{d}x} + \frac{\dot{m}_v}{u_g} \tag{25}$$

$$\frac{\mathrm{d}r_d}{\mathrm{d}x} = -\frac{\dot{m}_v}{\rho_d 4\pi r_d^2 n_d u_d} \tag{26}$$

$$\frac{\mathrm{d}u_d}{\mathrm{d}x} = -\frac{f_d}{\rho_d n_d \frac{4}{3}\pi r_d^3 u_d} \tag{27}$$

$$\frac{\mathrm{d}T_d}{\mathrm{d}x} = \frac{q_d - \dot{m}_v L}{\rho_d n_d \frac{4}{3}\pi r_d^3 u_d c_{v,d}} \tag{28}$$

$$\frac{\mathrm{d}Y_{g,k}}{\mathrm{d}x} = \frac{1}{\rho_g u_g}[\omega_k W_k + \dot{m}_v(Y_{d,k} - Y_{g,k})] \qquad k = 1, \ldots, K \tag{29}$$

where M and $\overline{W_g}$ are the Mach number and average molecular weight of the gas mixture, respectively.

The parameter S in the numerator of Eq. (22) consists of the energy source/sink terms due to wall drag, wall heat loss, droplet drag, droplet heat loss, and vaporization, respectively, as well as the chemical reaction term, which is the same as that in gas-phase detonation.[22] The detonation velocity D is the eigenvalue of this problem and can be obtained by matching the sonic point ($M \to 1$) and the point where all energy source terms balance ($S \to 0$), which constitutes the downstream boundary condition.[7]

Since all the parameters of the mixture ahead of the shock are known, the postshock parameters can be solved using the normal shock relations, with the assumption that the droplets maintain the same velocity and temperature in crossing the shock:

$$\rho_{g,1}u_{g,1} = \rho_{g,2}u_{g,2} \tag{30}$$

$$p_1 + \rho_{g,1}u_{g,1}^2 = p_2 + \rho_{g,2}u_{g,2}^2 \tag{31}$$

$$h_{g,1} + \tfrac{1}{2}u_{g,1}^2 = h_{g,2} + \tfrac{1}{2}u_{g,2}^2 \tag{32}$$

where the subscripts 1 and 2 respectively denote parameters before and immediately after the shock. The postshock parameters are used as the initial conditions of the preceding ordinary differential equations.

Results and Discussion

The preceding equations were solved numerically with a detailed reaction mechanism consisting of 41 species and 266 elementary reactions.[23] The parameters in Eq. (20) are $A = 4.02832$, $B = 1268.636$, $C = -56.199$, with T_d and $p_{f,s}$ having the units of K and bar, respectively[18]; Le and Pr were set to 1 and 0.72, respectively. The characteristic length l^* can be selected as the area-to-perimeter ratio of the cross section of a pipe, a duct, or a channel. Such a characteristic length allows the wall drag to be averaged on the cross section for practical one-dimensional approximation. In the calculations that follow, the characteristic length for a typical tube diameter of 3.81 cm is used such that the quenching behavior can be readily observed for normal loss coefficients. The results can be readily converted to those of other sizes and geometries by mapping the momentum and heat loss coefficients through the following relations:

$$C_{D,W}\big/l^* = C_{D,W}\big/l^{*'}, \qquad C_{H,W}\big/l^* = C_{H,W}\big/l^{*'} \tag{33}$$

Extensive exploration of the various parameters and subprocesses of the spray detonation structure and propagation showed that two aspects of the detonation dynamics are rather interesting and not readily anticipated, namely the effects of droplet size and prevaporization on detonation propagation and quenching. They are discussed in the following.

Effects of Droplet Size

The dependence of the computed detonation velocity on the momentum loss coefficient is shown in Fig. 2 for different droplet sizes and heat loss coefficients, with the initial conditions being $T_1 = 298.15$ K, $p_1 = 0.5$ atm, $\phi = 1$, and $\alpha = 1$. The heat loss coefficients are $C_{H,W} = 0$ and 0.01 for Figs. 2a and 2b, respectively.

Figure 2a shows that, as the drag coefficient approaches zero such that the system becomes lossless and corresponds to the CJ limit, the detonation velocity becomes progressively independent of the droplet size. Since droplet drag and heating still occur for vanishing momentum loss, the present result that the detonation velocity approaches the CJ velocity substantiates the concept that these "loss" processes are internal to the spray. That is, the loss is local and is recaptured by the gas as long as droplet vaporization is completed before the sonic point. Consequently, internal loss alone cannot extinguish a detonation wave.

When momentum loss to the environment is allowed, this "external" loss prolongs the ignition delay.[7] The lengthened ignition delay then leads to a corresponding increase in the integrated loss.

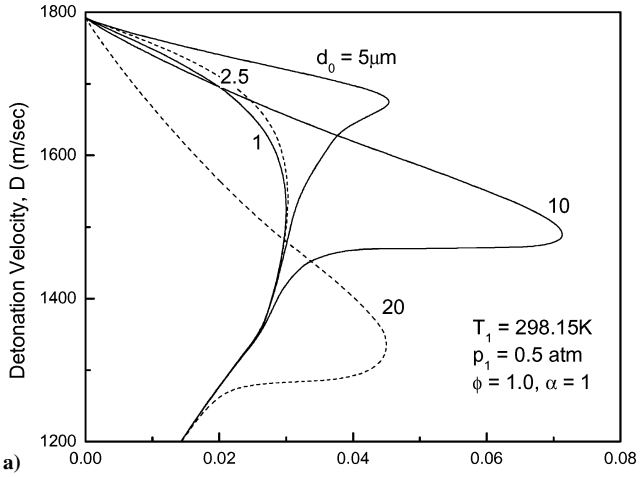

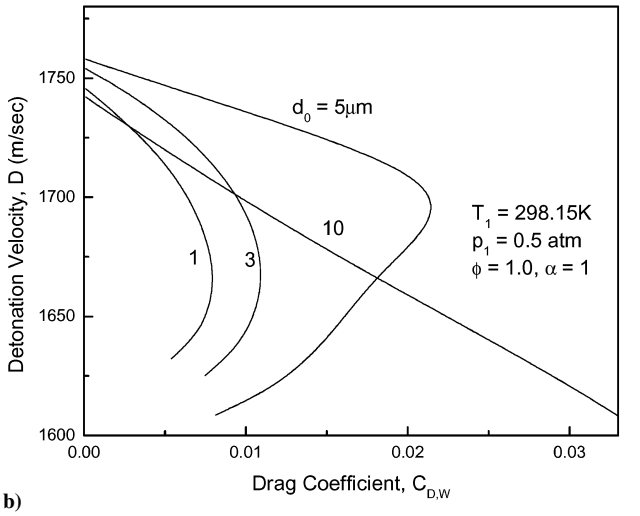

Fig. 2 Dependence of detonation velocity on momentum loss coefficient and droplet size for stoichiometric heptane/air spray mixture, with liquid fuel loading (defined as the fraction of total fuel in liquid phase) $\alpha = 1$, initial temperature 298.15 K, and initial pressure 0.5 atm: a) $C_{H,W} = 0$; b) $C_{H,W} = 0.01$.

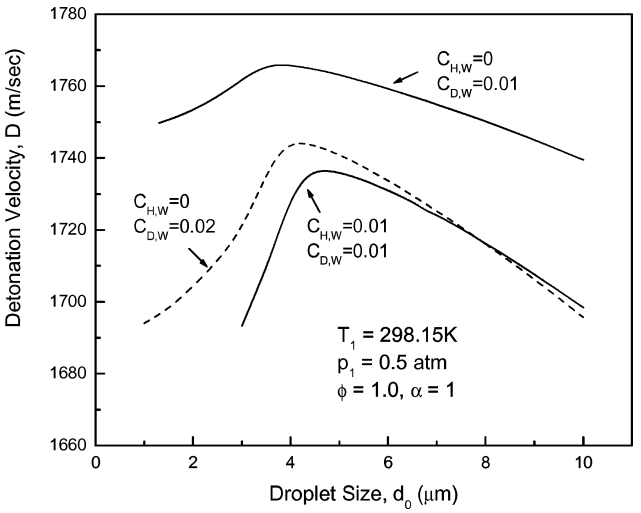

Fig. 3 Dependence of detonation velocity on droplet size with different momentum loss coefficient and wall heat loss coefficient, for stoichiometric heptane/air spray mixture, with liquid fuel loading $\alpha = 1$, initial temperature 298.15 K, and initial pressure 0.5 atm.

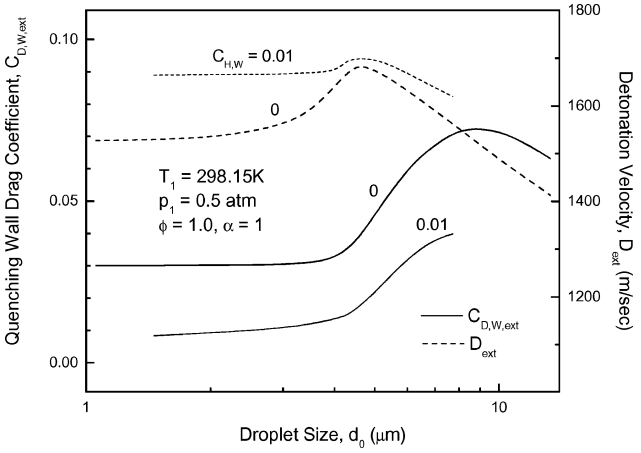

Fig. 4 Dependence of quenching momentum loss coefficient and the corresponding detonation velocity at the quenching point on droplet size, for stoichiometric heptane/air spray mixture with different heat loss coefficients, for liquid fuel loading $\alpha = 1$, initial temperature 298.15 K, and initial pressure 0.5 atm.

This reduces the detonation velocity, weakens the shock strength, and further increases the ignition delay. It is then clear that this nonlinear feedback mechanism could lead to detonation quenching. Consequently, for a given droplet size, the detonation velocity (on the upper branch of the solution curve) decreases with increasing drag coefficient until the wave is quenched at the turning point of the response curve, in accordance with the concept of Zeldovich[7] in identifying the turning point as the state of quenching.

The presence of droplet vaporization cools the gas and thereby further aggravates and sensitizes the ignition kinetics. However, unlike the case of particle-laden detonation,[9] for which the extent of reduction in detonation velocity increases monotonically with decreasing particle size, the variation is nonmonotonic for spray detonation. The quenching limit as indicated by the state of the turning point also shows a nonmonotonic dependence on the droplet size. Specifically, it is seen that, for a fixed momentum loss coefficient, the detonation velocity first increases as the droplet size increases, reaches a maximum value at a certain droplet size, and then decreases as the droplet size further increases. Approaching the limit of large droplet size, it is expected that the detonation velocity will decrease monotonically as the droplet size increases, as observed in previous experiments for droplet sizes of the order of hundreds of micrometers.[24]

A similar result is shown in Fig. 2b for nonadiabatic situations, with $C_{H,W} = 0.01$. It is seen that the quenching limits for the nonadiabatic curves in terms of, say, the momentum loss coefficient are much lower than those of the adiabatic cases due to heat loss to the wall. Furthermore, while detonation for droplet size less than 3 μm is beyond the quenching limit for the moderate momentum loss coefficient of 0.01, propagation is facilitated for mixtures with larger droplet sizes.

The aforementioned nonadiabatic behavior is demonstrated more clearly in Figs. 3 and 4. Specifically, Fig. 3 shows the nonmonotonic variation of the detonation velocity with the droplet size for various momentum and heat loss coefficients, demonstrating the existence of an optimum droplet size for maximum detonation velocity. Figure 4 plots the detonation velocity and the corresponding momentum loss coefficient at the quenching state, designated by the subscript ext, and again shows the nonmonotonic variation as well as the existence of an optimum droplet size for enhanced detonability.

The reason for this nonmonotonic response is shown in Figs. 5 and 6, in which the detonation structure in terms of the gas temperature and the droplet number density, size, and vaporization rate for different initial droplet sizes are compared. We first consider small droplets, with initial diameter of 1 μm. It is seen in Fig. 6a that the droplet number density continuously increases as the shocked gas flows downstream, which has been observed in previous theoretical and experimental work on spray and dust detonations.[20,25] This increase is caused by the drag acting on the droplet, rendering the flow more concentrated with droplets as it travels downstream. This point

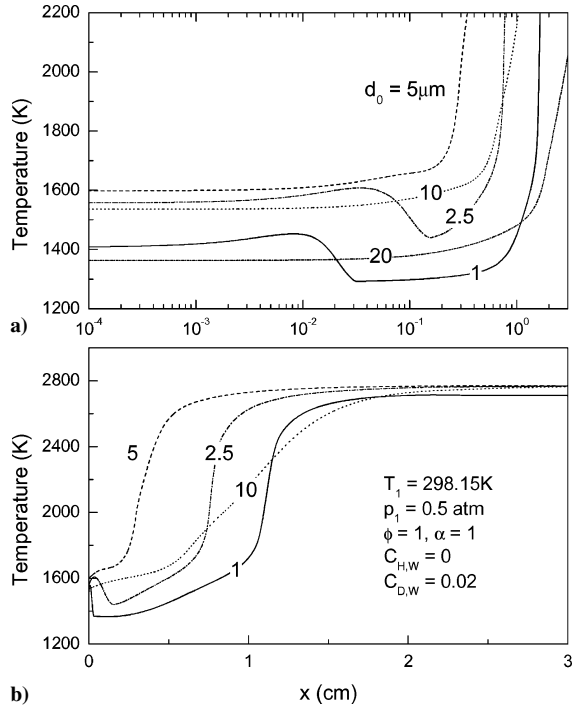

Fig. 5 Steady-state detonation temperature profiles of different droplet sizes for stoichiometric heptane/air spray mixture, with $\alpha = 1$, initial temperature 298.15 K, and initial pressure 0.5 atm, for fixed momentum loss coefficient $C_{D,W}$: a) log variation in x axis, b) linear variation in x axis.

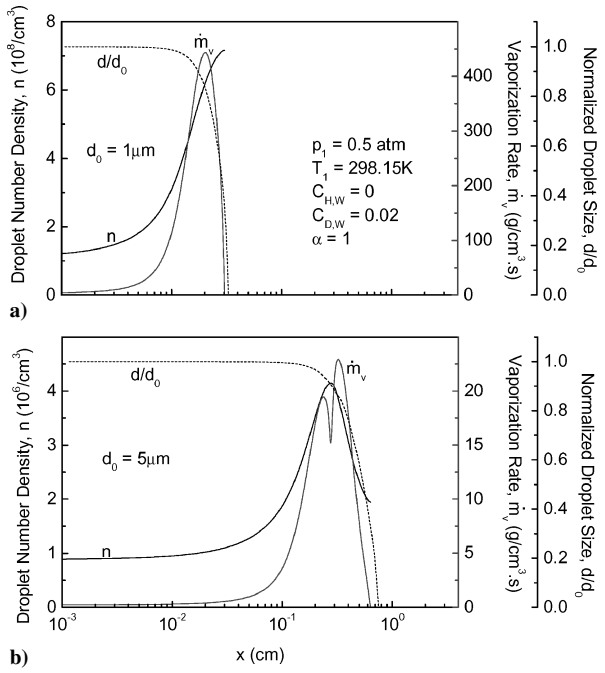

Fig. 6 Steady-state detonation profiles of droplet number density, volumetric vaporization rate, and normalized droplet size, for stoichiometric heptane/air spray mixtures, at initial temperature 298.15 K, initial pressure 0.5 atm, and droplet loading $\alpha = 1$, for droplet size a) $d_0 = 1$ μm, and b) $d_0 = 10$ μm.

is demonstrated in Fig. 5a, which shows that shortly downstream of the shock some chemical reaction is initiated, as indicated by the slight rise in the gas temperature. Since all the fuel is initially in the form of droplets ($\alpha = 1$), the amount of fuel participating in this reaction is all supplied by droplet vaporization. However, due to the increase in the droplet number density, the overall liquid vaporization rate is greatly increased after the initial droplet heating stage (Fig. 6a), causing a substantial cooling of the gas. Consequently, chemical reaction is suppressed and this first-stage ignition fails. The gas temperature then continuously decreases until the droplets are completely vaporized. The gas phase then undergoes a second ignition delay, under a lower temperature, and the ignition length is extended exponentially as a consequence. Ignition is eventually attained, as indicated by the temperature runaway.

Similar behavior is observed as the droplet size is increased to $d_0 = 2.5$ μm. Because the droplets experience a smaller drag effect, they are concentrated at a later stage, leading to more fuel vaporized and reacted and, hence, a larger increase in the gas temperature (Fig. 5a). This first-stage ignition, however, still fails when cooling due to vaporization being initiated. The second induction period is nevertheless shorter because the gas starts out with a higher temperature. The integrated external loss is then less, which results in a higher detonation velocity.

When the droplet size is increased to $d_0 = 5$ μm (Fig. 6b), the deceleration due to drag is very small and the first-stage thermal runaway is already sufficiently advanced that it cannot be suppressed by the cooling due to the concentrated vaporization. The first-stage ignition is therefore successful, with reduced ignition length and integrated heat loss and, consequently, increased detonation velocity. It is also of interest to note that the momentary dip in the vaporization rate shown in Fig. 6b is due to the diminishment of its convective augmentation, through the $0.276Re^{1/2}Pr^{1/3}$ term in Eq. (16), as the droplets travel almost in phase with the gas. Furthermore, the eventual reduction in the droplet number density, compared to the monotonically increasing trend for the 1-μm case, is due to the increase in gas velocity with significant chemical heat release, causing the droplet to lag behind the gas and, hence, diluting its concentration. The increased temperature due to thermal runaway is the major reason for the second peak in the vaporization rate.

Further increasing the droplet size increases the ignition delay again because vaporization becomes too slow such that the gas-phase reaction is "choked" and limited by the rate of droplet vaporization. This then leads to a fundamental change in the detonation structure, as shown in Fig. 5b, which is the same plot as Fig. 5a except the x variation is now linear to accentuate the differences in the structure for small and large droplets. It is seen that although the temperature increase is exponential-like for the small droplets, indicating Arrhenius sensitivity of the reactions, it is more gradual and in fact is somewhat linear for the larger droplets, indicating a substantially milder sensitivity in the reaction rate. The reaction is therefore choked for these situations, being controlled by the vaporization rate. This is demonstrated in Fig. 7, in which development of the local droplet loading ratio is plotted. It is seen that for smaller droplets this ratio is less than unity, indicating the presence of fuel

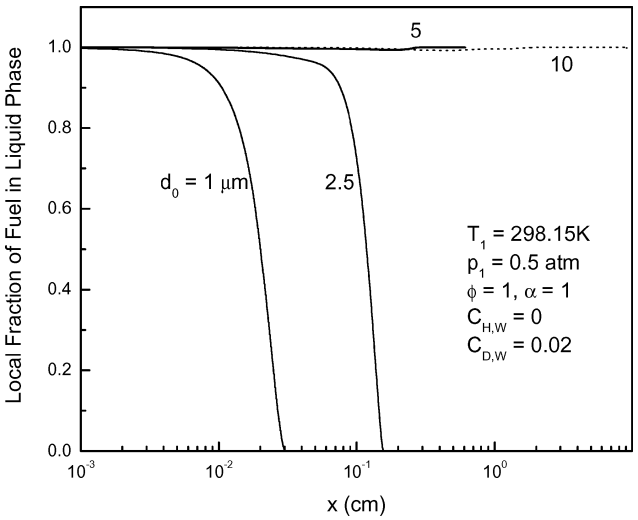

Fig. 7 Variation of local liquid fuel loading, defined as the fraction of total fuel in liquid phase, with the postshock space coordinate x, for different droplet sizes, with initial liquid fuel loading $\alpha = 1$, initial temperature 298.15 K, and initial pressure 0.5 atm ($C_{H,W} = 0$ and $C_{D,W} = 0.02$).

vapor which is needed to support the gas-phase Arrhenius reaction. However, for larger droplets, this ratio is basically unity, indicating the immediate consumption of any vapor that is released by the droplets.

Returning to Fig. 2, it is seen that moderately large droplets (e.g., $d_0 = 10\ \mu$m) can sustain higher quenching limits. The reason is that since the overall vaporization rate is now slower and, hence, exerts a greater influence on the rate of fuel consumption, the heat release rate becomes less sensitive to temperature through Arrhenius kinetics. This reduced sensitivity is substantiated by the extensive range of linearlike dependence of the detonation velocity reduction on the loss strength. Of course, when the droplet is too large (e.g., $d_0 = 20\ \mu$m), the "induction" length becomes excessively long and quenching is facilitated due to the correspondingly significant increase in the integrated loss.

Effects of Prevaporization

In the study of spray combustion there is always the interest of prevaporizing the fuel under the belief that processes involving droplet vaporization and burning would prolong the spray combustion time. To investigate the effects of fuel prevaporization on detonability, Fig. 8 shows the detonation velocity as a function of the momentum loss coefficient for droplet sizes of 1 and 10 μm, with various levels of liquid fuel loading, α. It is seen that, for the small droplet of 1 μm, prevaporization increases the detonation velocity and extends the detonability limit for both adiabatic and nonadiabatic cases, although the effect is relatively small. The reason for the facilitation is the reduced time needed for postshock vaporization. For larger droplets, however, this effect on the detonation velocity holds only for small drag coefficients. As the drag coefficient increases, dependence of the detonation velocity on the liquid loading varies nonmonotonically.

To understand this interesting behavior, the detonation structures for three different cases are compared: no liquid loading ($\alpha = 0$), maximum liquid loading ($\alpha = 1$) with small droplet size ($d_0 = 1\ \mu$m), and maximum liquid load with large droplet size

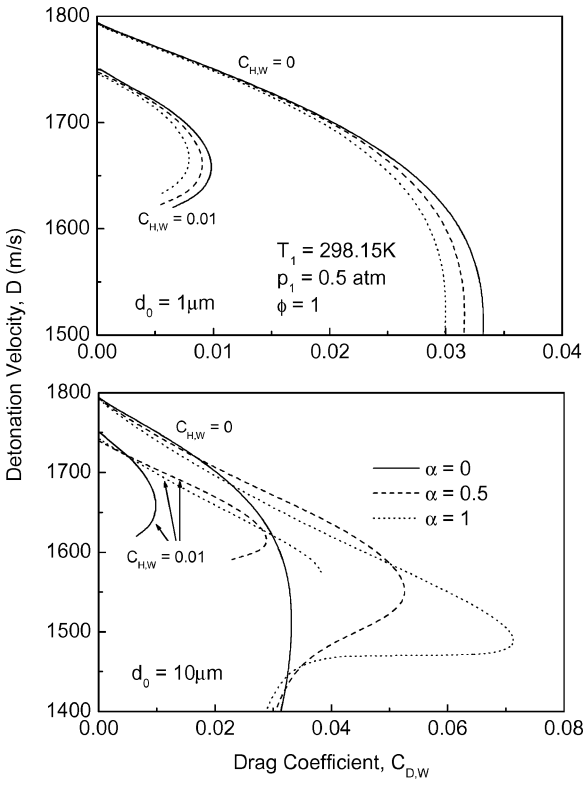

Fig. 8 Dependence of detonation velocity on momentum loss coefficient and droplet loading α for stoichiometric heptane/air spray mixtures at initial temperature 298.15 K, initial pressure 0.5 atm, and for droplet size a) $d_0 = 1\ \mu$m and b) $d_0 = 10\ \mu$m.

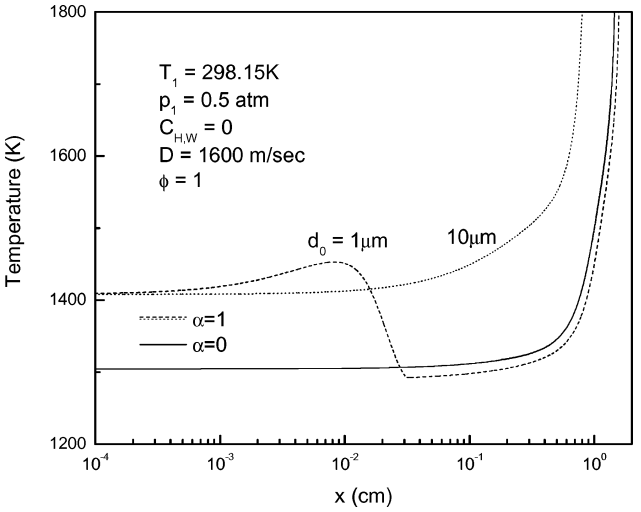

Fig. 9 Comparison of steady-state detonation structure of stoichiometric heptane/air spray mixtures for the case in which all the fuel is initially in the gaseous phase ($\alpha = 0$) and the cases in which all the fuel is in the liquid phase ($\alpha = 1$) but with different droplet sizes (1 and 10 μm), showing that the mixture with all liquid fuel has a higher postshock temperature than that with all fuel in gaseous phase.

($d_0 = 10\ \mu$m). Furthermore, it is important to account for the energy transferred from the gas phase to the latent heat of vaporization in the course of prevaporization. The effect can be assessed in the limits of isothermal and adiabatic freestreams, as follows.

We first study the isothermal situations, with $T_1 = 298.15$ K. Figure 9 shows that for the pure gaseous case ($\alpha = 0$) the temperature immediately downstream of the shock is about 100 K lower than the other two cases of maximum loading. The 1-μm-droplet case has a slightly longer induction length, compared to the gaseous case, due to the fast vaporization and, hence, failure of the first-stage ignition. However, the 10-μm-droplet mixture achieves runaway substantially earlier than the other two situations because it has a higher postshock temperature, as compared to the $\alpha = 0$ case. Furthermore, it also achieves runaway in the first ignition stage, as compared to the 1-μm case. Whereas the influence of droplet size on detonability has been explained in relation to Figs. 2, the cause for the different postshock temperatures for different amounts of liquid loading is identified as follows.

Figure 10 shows the normalized detonation Mach number, the heat capacity of the gas mixture before and after the shock, and the postshock temperature and pressure as functions of the liquid loading, calculated by using Eqs. (30–32). Normalizations of the Mach number and the specific heats are based on the states of the pure gas. It is seen that the postshock temperature and pressure exhibit opposite trends as the droplet loading changes, which cannot be explained based on constant-γ normal shock relations. To explain the higher p_2 with less loading, we note that the presence of a larger amount of vaporized fuel, which has a larger molecular weight than air, would reduce the upstream speed of sound, increase the shock Mach number, and consequently result in a greater degree of compression and, hence, a higher p_2. However, although the stronger shock also tends to increase the postshock temperature T_2, the larger specific heat associated with the many degrees of freedom of the larger fuel molecules has a greater effect on T_2, causing a net substantial reduction of this temperature. All of the preceding trends are clearly shown in Fig. 10. The preceding computation results, shown in Figs. 8–10, also agree with the experimental observation in previous work that the detonation velocity of fuel fog may be higher than that of the gas-phase detonation.[26]

Figure 11 shows effects of prevaporizations for an adiabatic upstream, using the enthalpy of the unvaporized case ($\alpha = 1$) as fixed values. It is seen that, for spray mixture with both small ($d_0 = 1\ \mu$m) and large ($d_0 = 10\ \mu$m) droplet sizes, propagation of the steady detonation wave through an adiabatically prevaporized mixture is only

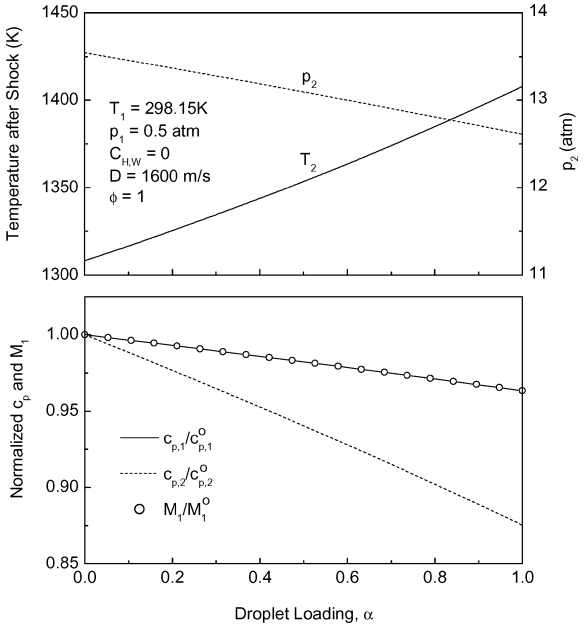

Fig. 10 Dependence of detonation Mach number, specific heat of gas mixture before and immediately after shock, temperature, and pressure immediately after shock, on droplet loading α for fixed detonation velocity, with $T_1 = 298.15$ K and $p_1 = 0.5$ atm.

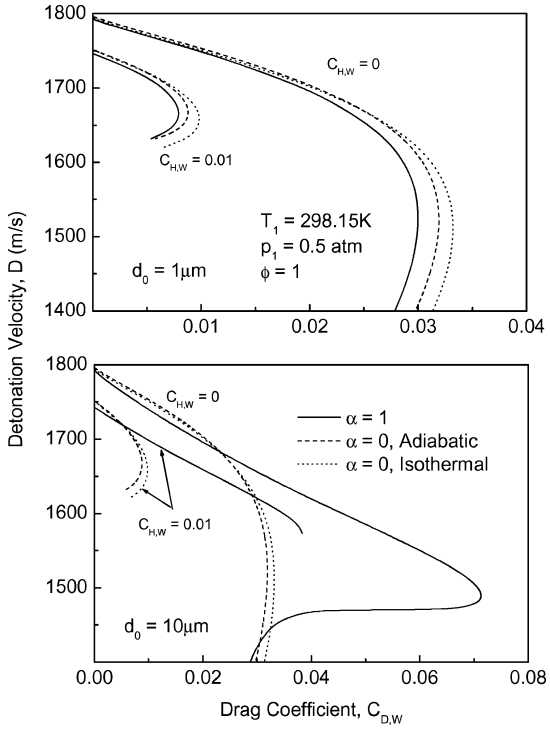

Fig. 11 Comparison of steady-state detonation structure of stoichiometric heptane/air spray mixtures for the cases in which all the fuel is totally prevaporized ($\alpha = 0$) in adiabatic and isothermal environment, with the case in which all the fuel is initially in the liquid phase ($\alpha = 1$) as reference, showing that the steady-state detonation velocity and the quenching limit only differ slightly between adiabatic and isothermal prevaporization cases.

slightly faster than that through an isothermal one for small wall drag coefficient. However, the quenching momentum loss coefficient for the adiabatic prevaporization case is only slightly smaller than that of the isothermal case for both small and large droplet sizes. The insensitivity of the detonation velocity to upstream adiabaticity vs isothermicity is due to the cancellation of two opposite effects. Specifically, by promoting isothermicity, the upstream temperature is increased. This, on the one hand, tends to increase the downstream temperature strictly due to shock jump considerations, whereas, on the other hand, it weakens the shock strength due to the increase in the speed of sound and, hence, decrease in the Mach number. The net effect is therefore small. The same consideration, though with opposite trend, can be extended to adiabatic situations. This result therefore implies that the effects of prevaporization on the detonability discussed earlier hold for isothermal, adiabatic, and the intermediate situations.

Conclusions

Through the present study, we have come to appreciate the richness in phenomena offered by the various heterogeneous droplet processes in spray detonation. Consequently we were able to identify, and explain, the possible existence of optimum droplet sizes and loadings for enhanced detonation propagation and the extension of quenching limits. These phenomena are consequences of the strong coupling among droplet size, vaporization, momentum, and heat loss and, as such, they would not have been captured had we made such conventional assumptions as in-phase velocities, d^2-law vaporization, and constant specific heats.

The present result, that there exists an optimum droplet size for detonation propagation such that propagation may be inhibited by both increasing and reducing the droplet size, is of particular interest. In this regard we note that, in the case of dust detonation, it was observed[27] that for a given dust loading it was more difficult to detonate a mixture with finer particle size. The reason given for this observation is similar to the present one.

We further note that although the study was conducted for the one-dimensional planar detonation in a tube which offers the crucial loss mechanism, the understanding gained herein can be readily transferred to the interpretation of the propagation and quenching of freely propagating curved detonation waves, because it has been well established that the effects of the momentum loss to the environment are dynamically similar to that due to the curvature of the wave.[7,10]

The identification of two modes of heat release, Arrhenius vs vaporization controlled, is particularly interesting because they depict two different detonation structures that are affected by the droplet size. Extension of the present study and understanding to other practical problems such as dust explosion of combustible materials is also warranted.

Acknowledgments

This research was initially supported by the Office of Naval Research and was completed under support by the Air Force Office of Scientific Research. We thank Yiguang Ju of Princeton University for helpful discussions.

References

[1]Dabora, E. K., "Fundamental Mechanisms of Liquid Spray Detonations," *Fuel-Air Explosions*, edited by J. H. S. Lee and C. M. Guirao, Univ. of Waterloo Press, Waterloo, ON, Canada, 1982, pp. 245–264.

[2]Sichel, M., "The Detonation of Sprays: Recent Results," *Fuel-Air Explosions*, edited by J. H. S. Lee and C. M. Guirao, Univ. of Waterloo Press, Waterloo, ON, Canada, 1982, pp. 265–302.

[3]Smirnov, N. N., and Tyurnikov, M. V., "A Study of Deflagration and Detonation in Multiphase Hydrocarbon—Air Mixtures," *Combustion and Flame*, Vol. 96, Nos. 1–2, 1994, pp. 130–140.

[4]Smirnov, N. N., Zverev, N. I., and Tyurnikov, M. V., "Two-Phase Flow Behind a Shock Wave with Phase Transition and Chemical Reactions," *Experimental Thermal and Fluid Science*, Vol. 13, No. 1, 1996, pp. 11–20.

[5]Strehlow, R., *Combustion Fundamentals*, McGraw–Hill, New York, 1984.

[6]Williams, F. A., "Detonation and Two Phase Flow," *Progress in Astronautics and Rocketry*, edited by S. S. Penner and F. A. Williams, Vol. 6, Academic, New York, 1962, pp. 99–114.

[7]Zeldovich, Ya. B., Gelfand, B. E., Kazhdan, Ya. M., and Frolov, S. M., "Detonation Propagation in a Rough Tube Taking Account of Deceleration and Heat Transfer," *Combustion, Explosion, and Shock Waves*, Vol. 23, No. 3, 1987, pp. 342–349.

[8]Kusharin, A. Y., Agafonov, G. L., Popov, O. E., and Gelfand, B. E., "Detonability of H_2/CO/CO_2/Air Mixtures," *Combustion Science and Technology*, Vol. 135, Nos. 1–6, 1998, pp. 85–98.

[9]Teodorczyk, A., "Structure and Velocity Deficit of Gaseous Detonation in Rough Tubes," Dynamic Aspects of Detonations, edited by A. L. Kuhl, J.-C. Leyer, A. A. Borisov, and W. A. Sirignano, Vol. 153, Progress in Astronautics and Aeronautics, AIAA, Washington, D.C., 1993, pp. 405–424.

[10]Ju, Y., and Law, C. K., "Propagation and Quenching of Detonation Waves in Particle Laden Mixtures," *Combustion and Flame*, Vol. 129, No. 4, 2002, pp. 356–364.

[11]Fan, B. C., and Sichel, M., "A Comprehensive Model for the Structure of Dust Detonations," *Proceedings of the Combustion Institute*, Vol. 22, 1988, pp. 1741–1750.

[12]Lee, D., and Sichel, M., "The Chapman-Jouguet Condition and Structure of Detonation in Dust-Oxidizer Mixtures," Dynamics of Explosions, edited by J. R. Bowen, J.-C. Leyer, and R. I. Soloukhin, Vol. 106, Progress in Astronautics and Aeronautics, AIAA, New York, 1985, pp. 505–521.

[13]Law, C. K., "A Theory for Monodisperse Spray Vaporization in Adiabatic and Isothermal Systems," *International Journal of Heat and Mass Transfer*, Vol. 18, No. 11, 1975, pp. 1285–1292.

[14]Law, C. K., "Adiabatic Spray Vaporization with Droplet Temperature Transient," *Combustion Science and Technology*, Vol. 15, Nos. 1–2, 1977, pp. 65–74.

[15]Liu, C. C., and Lin, T. H., "The Interaction Between External and Internal Heat Losses on the Flame Extinction of Dilute Sprays," *Combustion and Flame*, Vol. 85, Nos. 3–4, 1991, pp. 468–478.

[16]Eidelman, S., and Burcat, A., "Evolution of a Detonation Wave in a Cloud of Fuel Droplets: Part I. Influence of Igniting Explosion," *AIAA Journal*, Vol. 18, No. 9, 1980, pp. 1103–1109.

[17]Law, C. K., "Recent Advances in Droplet Vaporization and Combustion," *Progress in Energy and Combustion Science*, Vol. 8, No. 3, 1982, pp. 171–201.

[18]Willingham, C. B., Taylor, W. J., Pignocco, J. M., and Rossini, F. D., "Vapor Pressures and Boiling Points of Some Paraffin, Alkylcyclopentane, Alkylcyclohexane, and Alkylbenzene Hydrocarbons," *Journal of Research of the National Bureau of Standards*, Vol. 35, No. 3, 1945, pp. 219–244.

[19]Smirnov, N. N., "Combustion and Detonation in Multi-Phase Media, Initiation of Detonation in Dispersed-Film Systems Behind a Shock Wave," *International Journal of Heat and Mass Transfer*, Vol. 31, No. 4, 1988, pp. 779–793.

[20]Smirnov, N. N., Nikitin, V. F., and Kulchitsky, A. V., "Detonation Initiation in Pulse Detonating Devices," *Proceedings of the 13th ONR Propulsion Meeting*, Office of Naval Research, Arlington, VA, 2000, pp. 213–232.

[21]Kulchitskii, A. V., and Smirnov, N. N., "Accounting for Non-equilibrium Effects at Evaporation of a Solution Droplet," *Journal of Engineering Thermophysics*, Vol. 10, No. 4, 2000, pp. 293–314.

[22]Mitchell, R. E., and Kee, R. J., "SHOCK: A General Purpose Computer Code for Predicting Chemical Kinetic Behavior Behind Incident and Reflected Shocks," Sandia National Lab., Livermore, CA, Rept. 82-8205, 1982.

[23]Held, T. J., Marchese, A. J., and Dryer, F. L., "A Semi-Empirical Reaction Mechanism for n-Heptane Oxidation and Pyrolysis," *Combustion Science and Technology*, Vol. 123, Nos. 1–6, 1997, pp. 107–146.

[24]Dabora, E. K., Ragland, K. W., and Nicholls, J. A., "Dropsize Effects in Spray Detonations," *Proceedings of the Combustion Institute*, Vol. 12, 1968, pp. 19–26.

[25]Korobeinikov, V. P., "On Arising in Dusty Gas of Zones with High Concentration of Particles," *Archivum Combustionis*, Vol. 9, Nos. 1–4, 1989, pp. 149–152.

[26]Boween, J. R., Ragland, K. W., Steffes, F. J., and Loflin, T. G., "Heterogeneous Detonation Supported by Fuel Fogs or Films," *Proceedings of the Combustion Institute*, Vol. 13, 1970, pp. 1131–1139.

[27]Lee, F. P., Kauffman, C. W., Sichel, M., and Nicholls, J. A., "Detonability of RDX Dust in Air Oxygen Mixtures," *AIAA Journal*, Vol. 24, No. 11, 1986, pp. 1811–1816.